The Iraqi Journal for Mechanical and Material Engineering, Vol.42, No.1, May. 2025

IMPACT OF INCLINATION AND V-SHAPED RIBS ON FREE CONVECTION FROM INCLINED SQUARE AIR DUCT SUBJECTED TO LATERAL THERMAL FLUX: AN EXPERIMENTAL STUDY

Eman Ali Mohammed[1] **Rafel Hekmat Hameed[2]**
eng556.eman.ali@student.uobabylon.edu.iq eng.rafel.hekmat@uobabylon.edu.iq
[1] College of Engineering- Department of Mechanical Engineering - University of Babylon- Wasit – Iraq
[2] College of Engineering- Department of Mechanical Engineering - University of Babylon- Hilla - Iraq

ABSTRACT
This study experimentally investigates natural convection heat transfer in an inclined rectangular duct with a square cross-section. The effects of inclination angles (30°, 45°, and 60°) and v-shaped ribs on the performance of heat transfer are examined under steady-state conditions at a heat flux varying from 63.45 W/m² to 634.52 W/m². The modified average Rayleigh number (Ra*) ranges from 11.5×10^6 to 10.56×10^7 and a. The results indicate that increasing the inclination angle and adding ribs significantly enhance natural convection by intensifying turbulence and disrupting the thermal boundary layer. With increasing inclination angle and the introduction of V-shaped ribs, at 30°, 45°, and 60°, the ribbed duct showed heat transfer enhancements of 21.7%, 32.17%, and 48.15%, respectively, compared to the smooth duct. Furthermore, the local heat transfer increases with inclination angle and adding ribs.

Keywords: Inclination angle, Natural convection, 45ºV-shaped ribs, lateral heat flux, Modified number of Rayleigh.

NOMENCLATURES AND SYMBOLS

h	Coefficient of heat transfer, $(\frac{W}{m^2.K})$
$Nu_{(av)}$	Average number of Nusselt
T	Temperature, C°
q	Heat flux, $\frac{w}{m^2}$
As	Area, m^2
k	Thermal conductivity, $(W.\ m^{-1}\ .\ k^{-1})$
g	gravity acceleration,(m/s^2)
Ra^*	Modified number of Rayleigh

Received: February 10, 2025.
Accepted: March 10, 2025.

Pr	Prandtl number
D_h	hydraulic diameter,(m)
e	Rib height, (m)
e/D_h	Relative roughness height
S	Spacing between ribs, (m)
α	Thermal diffusivity ($m^2 . s^{-1}$)
θ	Inclination angle, (degree)
β	Thermal expansion coefficient (k^{-1})
s	surface
x	local
a	ambient
av	average
b	bulk
Θ°	Ribs attack angle

INTRODUCTION

Natural convection that arises naturally as a consequence of the buoyant force is often preferred to forced convection due to its low operational noise level, simplicity, ease of maintenance, and low cost due to the lack of mechanical moving parts like blowers, pumps, and fans, as stated by Naje and Hasan [2022]. Therefore, understanding this phenomenon is important due to its wide use for different engineering purposes, like system cooling for electrical and electronic components, solar air heaters, and heat exchangers.

Numerous studies have analyzed how the inclination angles of ducts affect the performance of natural convection rates. Moawed and Ibrahim [2009] investigated elliptical tubes inclined between $15^o$and 90^oover a Rayleigh number range of $65 \times 10^{4}$to 11.3×10^7. They found that surface temperatures peaked at the tube's midpoint, and the local number of Nusselt increased with larger axial ratios and higher inclination angles. Kalendar et al., [2010] analyzed square cylinders with various aspect ratios inclined from 0^o to 180^o. Their results indicated that average Nu increased with decreasing aspect ratios and became more dependent on inclination at Rayleigh numbers above 10^4.

Gharehghani et al. [2010] examine the effect of inclination angles, diameter, and length on free convective from a horizontal, inclined, and vertical duct. The tilt angles ranged from 0^o to 90^o for five different heat fluxes, from a minimum of 780 w/m^2 to a maximum of 4800 w/m^2. Experiential outcomes indicated that, at a constant Ra number, increasing either the diameter or length of the duct brings a minimize in the Nu number, and heat transfer efficiency declined at inclinations greater than 15^o.

Mohammed et al, [2011] discuss the influence of surface heat flux and angles of inclination of 0^o, 30^o , 60^o and 90^o on the distributions of temperature and local Nu number along the inclined circular duct surface at heat fluxes changing from 92 w/m^2 to 487w/m^2.

The findings demonstrate that the increment in thermal flow and the transition of the inclination from a vertical to a horizontal situation cause an increase in the transfer of heat.

Al-Kayiem and Yassen [2014] identified 50^oas the optimal inclination for heat transfer in rectangular ducts used in solar heaters, with Rayleigh numbers between 6×10^4 and 28×10^4. Similarly, Ghani and Salman[2014] demonstrated that higher inclinations (0^o-90^o) and increased heat flux enhanced both local and mean Nu in inclined annuli. Bhushan and Reddy[2015] observed a linear relationship between Nu and Rayleigh numbers (Ra*) in the laminar regime (Ra*<10^9) for an inclined square duct, with superior Nu values compared to a vertical duct.

Abidi-Saad et al.[2016] found that square ribs placed at the top of vertical channels improved heat transfer by up to 27% at moderate numbers of Rayleigh. Gilani et al. [2016] showed that conical pins on solar collector plates enhanced Nu by 41%, with 50° being the most efficient inclination angle.

Ali Mohammed[2017] made an investigation on the transfer of free convective from an inclined square duct with five varying cross-sections and inclined at 30, 45 and 60 degrees at fixed flux of heat with a range of modified Ra numbers ($4\times 10^4 \leq Ra^* \leq 1\times 10^8$). The results showed that as the modified number of Rayleigh increased, so did the number of Nusselt, indicating a mild dependence on the inclination angle. Heat transfer was primarily laminar, decreasing with side length.

Nemade and Patil [2017] compared the performance of natural convection for cylindrical and square rods tilted from 0^o to 90^o with an increment of 15^o. They found that maximum heat transfer occurred at 45^o for square rods. Abdelatief and Omara[2018] examined the free convection heat transmission through a square tube with a roughened inner surface at different inclination angles (0^o, 30^o, 45^o, 60^o, 75^o, and 90^o) with a heat flux between 51 w/m^{2}and 1198 w/m^{2}and Ra number ranges of 8.92 $\times 10^5$ to 1.1×10^7. Depending on Ra number values, results revealed that roughened square tubes achieved higher Nu values than smooth tubes, particularly at $\theta = 0^o$.

Shehab S. N.[2021] examined the impact of 0°, 15°, and 45° inclination of triangular channels under thermal fluxes ranging from 2×10^2 w/m^2 to 10^3 w/m^2 and Rayleigh numbers between 10^6 and 10^7. The findings revealed that 45^o inclination improved airflow efficiency by 16–20% compared to horizontal orientations.

Shehab S. N.[2022] investigated the impact of baffle arrangements on free convection heat transfer in a square cross-section duct. The duct was heated at several heat fluxes (500, 1000, 1500, and 2000 w/m^2). The study found that a staggered perforated baffle arrangement was the most effective in enhancing the rate of heat transmission in terms of Nusselt number, which was higher than the inline and staggered arrangements under similar conditions.

Al-Suhaibani et al. [2024] investigate how tilt angles of 30°, 45°, and 60° affect natural convection heat transfer in an array of square cylinders. Results indicate that lower angles enhance Nusselt numbers, particularly at high modified Rayleigh numbers, compared to higher angles.

The comparison between smooth and rough ducts provides valuable insights into the effects of surface modifications on convection's natural heat performance. Therefore, the current research seeks to analyze and improve natural convection heat transfer in an inclined duct by adding 45-degree ∨-shaped ribs on the right side wall of the square duct and comparing the result with the smooth duct.

EXPERIMENTAL SETUP

Figure (1) displays a schematic diagram of the experiential equipment setup. The experimental setup involves a rig to analyze the impact of different inclination angles and 45-degree ∨-shaped ribs on natural heat transfer convection performance. The main component of the rig is an aluminum duct with a square cross-section, measuring 200 cm in length, 40 cm in height, and 0.3 cm in thickness, insulated with glass wool. The side wall of the duct is slidable to facilitate the change of the smooth wall with the ribbed wall. A lever fixed to the horizontal frame was used to regulate the inclination of the square duct. The needed inclination angle was obtained by converting the lever's location to a, b, or c, as shown in Figure (2). The nine ∨-shaped aluminum ribs feature a 45-degree attack angle and a triangular cross-section with a rib pitch-to-rib height ratio of 5 (S/e=5) and the rib's altitude-to-duct hydraulic diameter ratio is 0.1 (e = 0.1 Dh). These ribs are attached to the heated right side wall of the duct using rivet screws, as shown in figure (3). The configuration of the ribs and their dimensions are illustrated in figure (4).

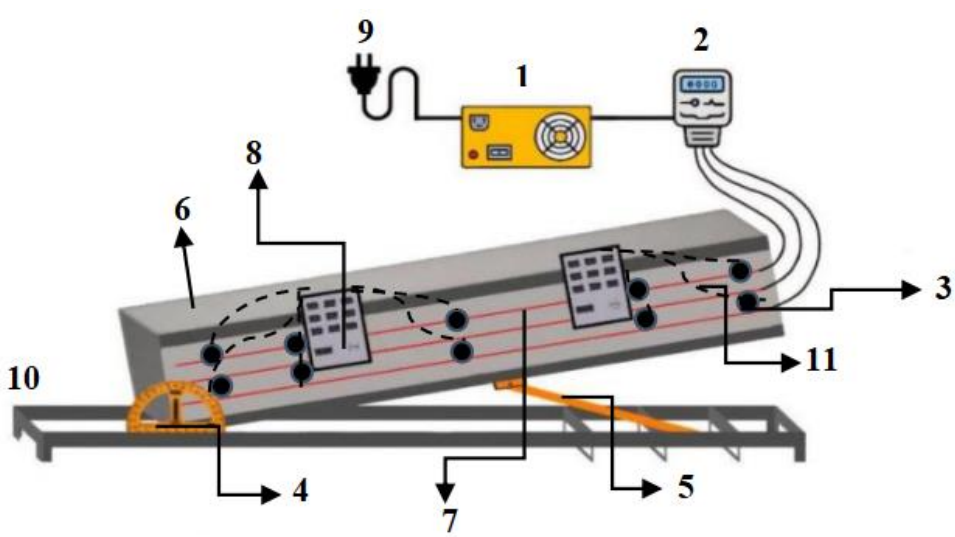

Fig.(1) Test rig schematic

1.Power supply 2. Power analyzer 3. Thermocouple 4. Protractor
5. lever to change the inclination angle 6. Duct 7. Heaters 8. Double digital Temperature Indicator Screen 9. Electrical source 10. Frame 11. Thermocouples wire

The heating of the duct was achieved using three 1500 W straight rod heaters, each 8 mm in diameter, to ensure uniform heat distribution. A variable-voltage device controls the heaters, providing a voltage range of 0-260 volts. A digital power analyzer LUTRON model (DW-6091) with a maximum current (10 A) and a maximum voltage (600 V) is employed to convert the analog voltage signals from the power supply into readable digital data. Thus, the heat flow values are (63.45-634.52) w/m^2, which are obtained by dividing the values of supplied power over the surface area of the sample.

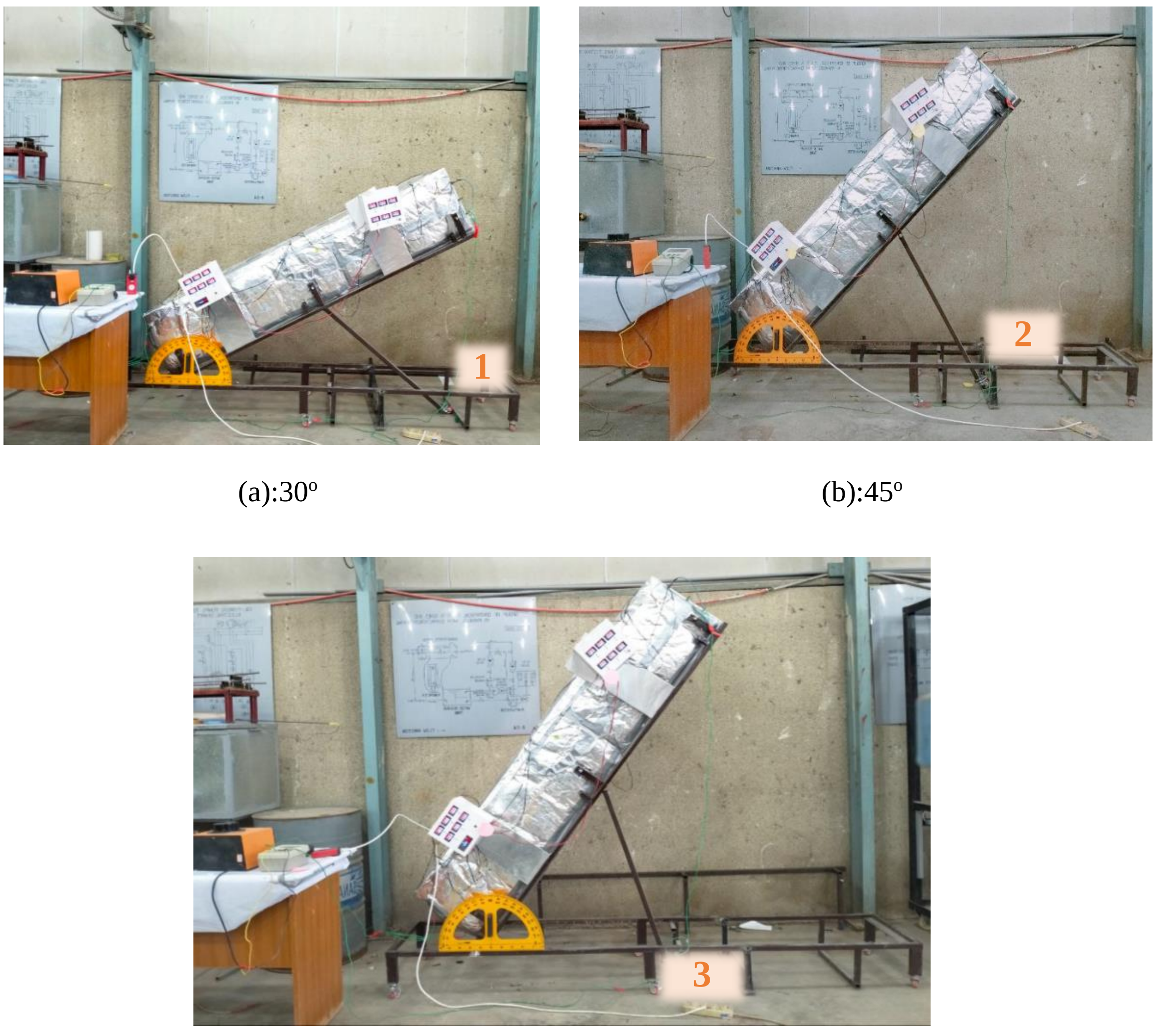

(a):30°

(b):45°

(c):60°

Fig. (2) Test rig Photography at different θ

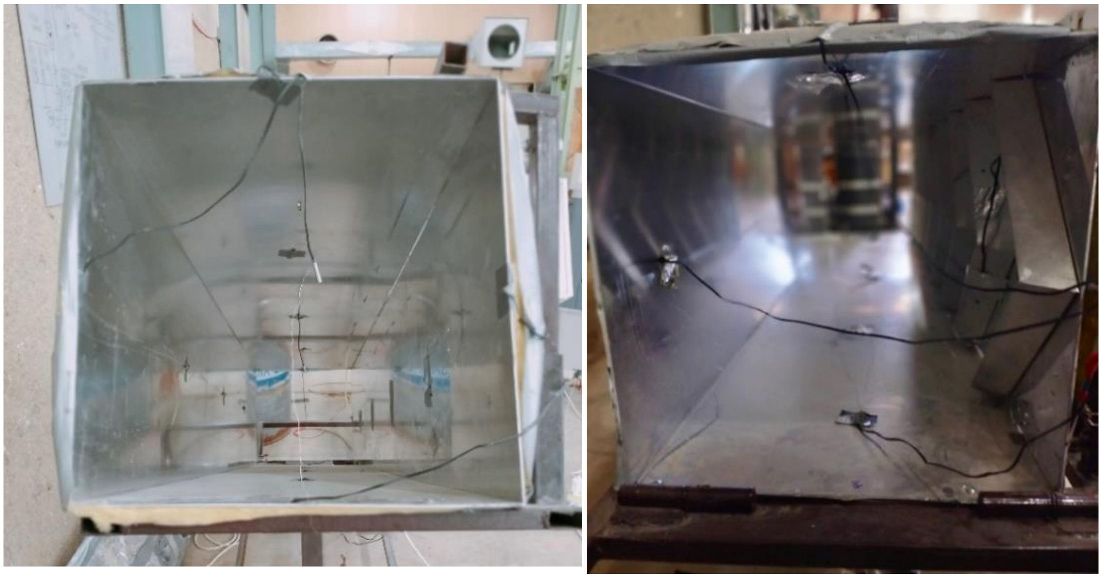

(a) (b)

Fig.(3)Duct cross section (a):Smooth side (b):Ribbed side

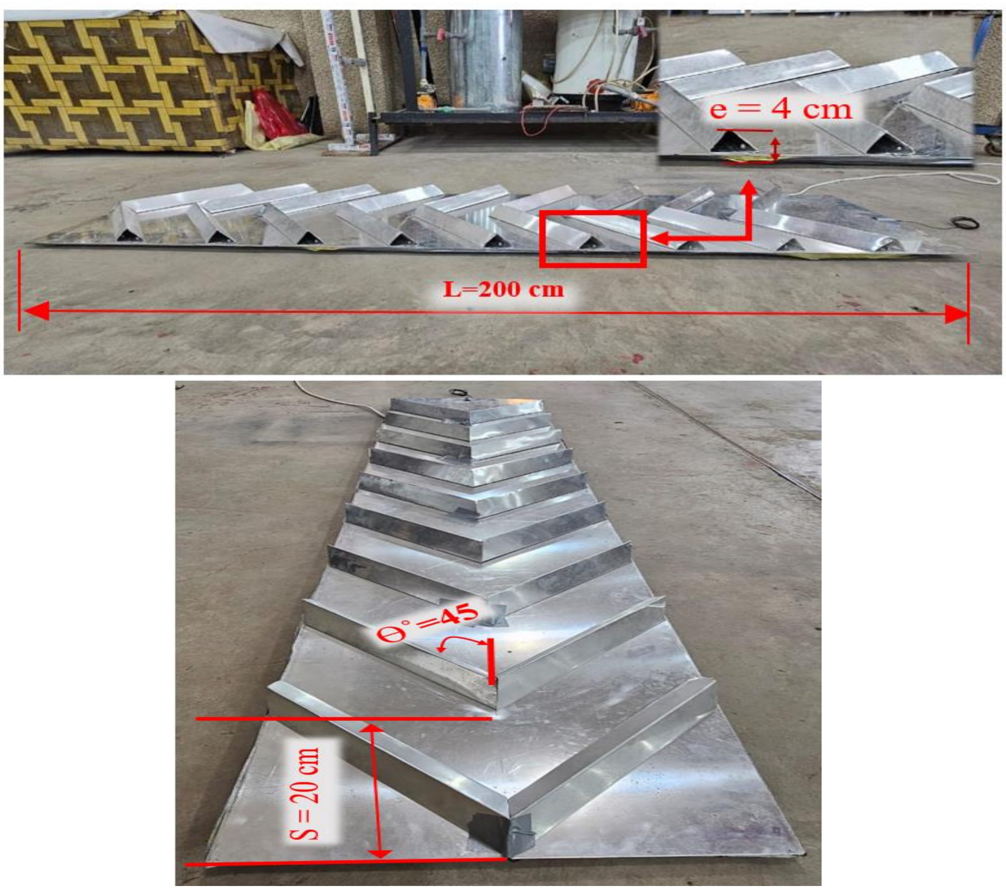

Fig.(4) Geometry and dimensions of the ribs

A double-display LED digital temperature indicator with a metal probe is used as a temperature indicator, as displayed in Figure (5-a). Twenty-two calibrated K-type thermocouples are employed for the temperature measurements; three of them are utilized to determine the entrance, exit, and center bulk air temperatures, and the others were distributed on the inner surface of the duct as shown in Figure (6). These thermocouples are fixed to the duct's internal surface using heat-resistant thermal tape, which can endure temperatures of up to 300C^{o} as shown in figure(5-b).

(a)

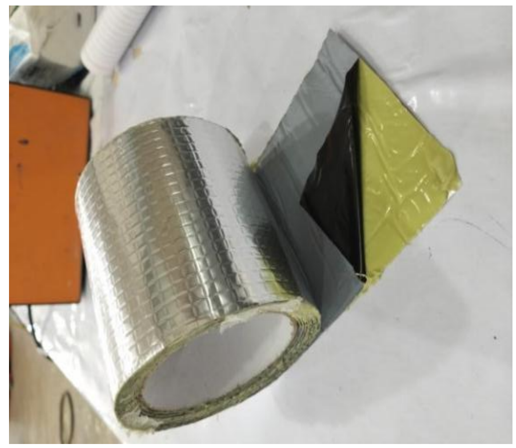

(b)

Fig.(5) a: Double-display LED digital temperature indicator, b:Thermal tape

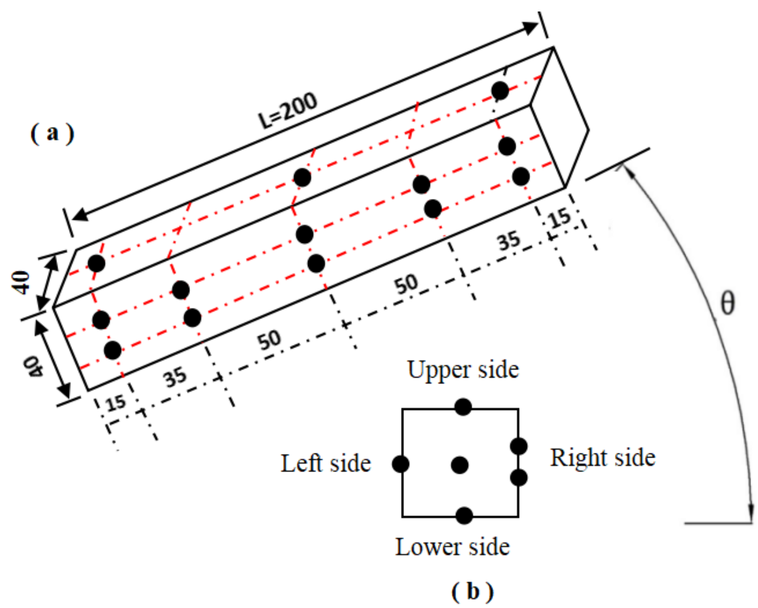

Fig. (6). Thermocouples distribution (a): inside duct surface (b): Duct cross-section (All dimensions in cm).

Experimental Procedure

Two tests are performed to examine and analyze the impact of the inclination angle and 45-degree V-shaped ribs on the rate of heat transmission through an inclined open-ended square duct at a uniform heat flow. Six several thermal fluxes, such as (63.45, 126.9, 253.81, 380. 71, 507.61 and 634.52 w/m^2) are utilized. The steps of tests can be summed up as follows:

1. Set the inclination angle to 30^o by fixing the movable lever at position1, as shown in Fig. (2-a).
2. Use the on/off switch to operate the digital temperature recorder.
3. Adjust the voltage and current using a voltage regulator to obtain the thermal flux of 63.45 W/m^2.
4. Thermocouple readings, voltage and current values have been recorded after 50 min, where the steady-state has been reached.
5. Iterate the same steps for another thermal flux and another inclination angle.
6. Iterate the above steps for the inclined ribbed duct.

THERMOCOUPLES CALIBRATION

Thermocouples used in this work were calibrated with the readings of the calibrated mercury thermometer at different water temperatures as reference points as mentioned by Hisham, S. H. [2023]. The calibration results are shown in table (1) and figure (7). Calibration was performed by immersing the thermocouple and mercury thermometer together in boiling water at the same time to record the readings and then repeating the process using hot, warm, cold and iced water. Pictures of the calibration procedure are included in Appendix A.

Table (1) calibration results.

T (C^o)	Thermocouple Temperature reading	Thermometer Temperature reading
Iced water	-3	-3
Cool water	5.5	5
warm water	31.3	31
Hot water	73.2	73
Boiling water	81.4	81

For adjusting the measured temperature measurements, a polynomial equation is derived:

$$T_{re}= 1.35 \times10^{-5}\, T^3_{calib} - 1.55\times10^{-3}\, T^2_{calib} + 1\ .04\, T_{calib} + 0.134 \qquad (1)$$

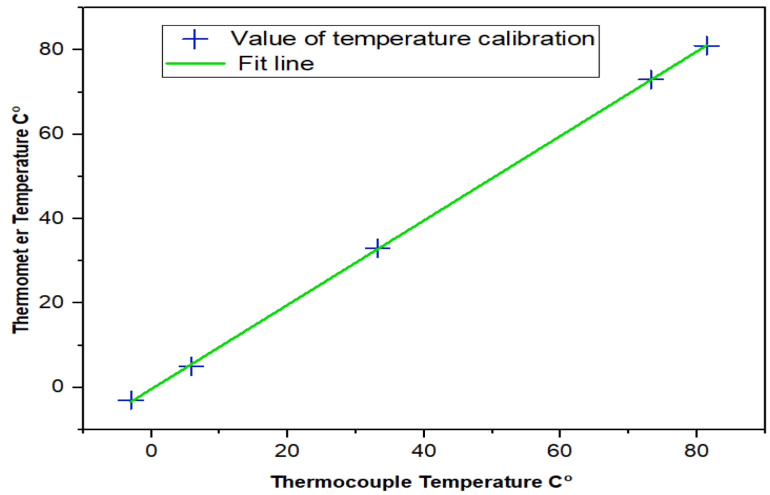

Fig. (7) Curve of temperature calibration

REDUCTION OF THE EXPERIMENTAL DATA

1. Coefficient of Heat Transfer:

The local coefficient of heat transmission (h_x) is can obtained by [Cengel,Y. A. , 2002] as follows:

$$h_x \frac{q}{(Tsx-Ta)} \quad ,(x=1,2,\ldots..,5) \tag{2}$$

Where:

T_{sx}: local Temperature

q: flux of heat is given by:

$$q = \frac{V.I}{As} \tag{3}$$

Where:

$As = D_h . L$

I : Current

V: voltage

T_b: is the he average of inlet and outlet bulk temperatures can calculated [Baskaya, S. et al., 1999] as:

$$T_b=\left(\frac{Tin+Tout}{2} \right) \tag{4}$$

All the properties of air were evaluated at the film temperature [Holman, J. P., 2010]as:

$$T_f = \frac{(Ts+T_b)}{2} \tag{5}$$

2. Number of Nusselt:

Based on the average coefficient of heat transfer, the average value of the Nu number can be determined as follows [Bejan, A., 2013]:

$$Nu_{av} = \frac{h_{av}.D_h}{k} \tag{6}$$

Where:

$$D_h = \frac{4\ As}{Pw}$$

h_{av} : is average coefficient of heat transfer given by as follows [Nemade, P. D. and Patil, D. R. K., 2017]:

$$h_{av} = \sum_{x=1}^{5} h_x / 5 \tag{7}$$

3.Rayleigh number:

The average value of the Ra^* number can be determined as follows [Bhushan, T. V. S. M. R. and Reddy, K. V. K., 2015]:

$$Ra^*_{av} = (g.\beta.\cos\theta.(Ts_{av} - T_a).Pr.{D_h}^3)/\nu^2 \tag{8}$$

Where:

Ts_{av} : Average surface temperature given by:

$$Ts_{av} = \int_0^L T_{sx}\, dx \tag{9}$$

ν: Kinematic viscosity($\frac{m^2}{s}$)

Pr: Prandtl number

Estimating Uncertainty

The term measurement mistake refers to the variance between reported and real values. It is not easy to determine the true quantity from a collection of readings, so while presenting experimental results, it is essential to compute an appropriate level of uncertainty. The standard uncertainty (S.U) may be computed for any collection of data by the equation detailed by Bell [2001] as:

$$S.U. = \frac{S.D.}{N} \tag{10}$$

Where:

N: is the overall number of measurement in each case.

S.D.: is the standard deviation which is calculated as:

$$S.D. = \sqrt{\frac{\sum_{I=i}^{N}(xi-xm)^2}{(N-1)}} \tag{11}$$

Where: x_m is the mean reading of temperature in each case is repeated (N) time and calculated as:

$$x_m = \frac{1}{N}\sum_{i=1}^{N} xi \qquad , (N=2) \tag{12}$$

xi: is represented the values for measurements temperature or any function measured in each case.

The overall standard uncertainty in temperature was calculated to be 0.127.

RESULTS

Impact of Inclination and Ribs on the Temperature Distribution

Figure (8) shows the variation of a temperature difference (Tsx - Ta) along a smooth and ribbed duct at different heat fluxes (from 63.45 w/m^2 to 634.52 w/m^2) and inclination angles (30^o, 45^o, and 60^o). In smooth ducts, the temperature difference trend demonstrates that as the axial distance increases, the temperature difference also increases, reaching a peak at the duct outlet. This is due to free convection in ducts, where the thermal boundary layer thickens due to air viscosity, while the thin boundary layer near the inlet results in lower temperature differences. Higher thermal flux values increase surface temperature due to more energy input, resulting in a higher temperature difference for a constant axial distance. However, increasing the inclination angle (θ) reduces the temperature difference, as buoyancy-driven convection enhances airflow and heat transfer. When the ∨-shaped ribs are introduced, they act as flow disruptors, generating turbulence and vortices that break up the thermal boundary layer. This disruption allows cooler air to interact more effectively with the heated surface, improving convective heat transfer and leading to a lower surface temperature as compared to the smooth duct .

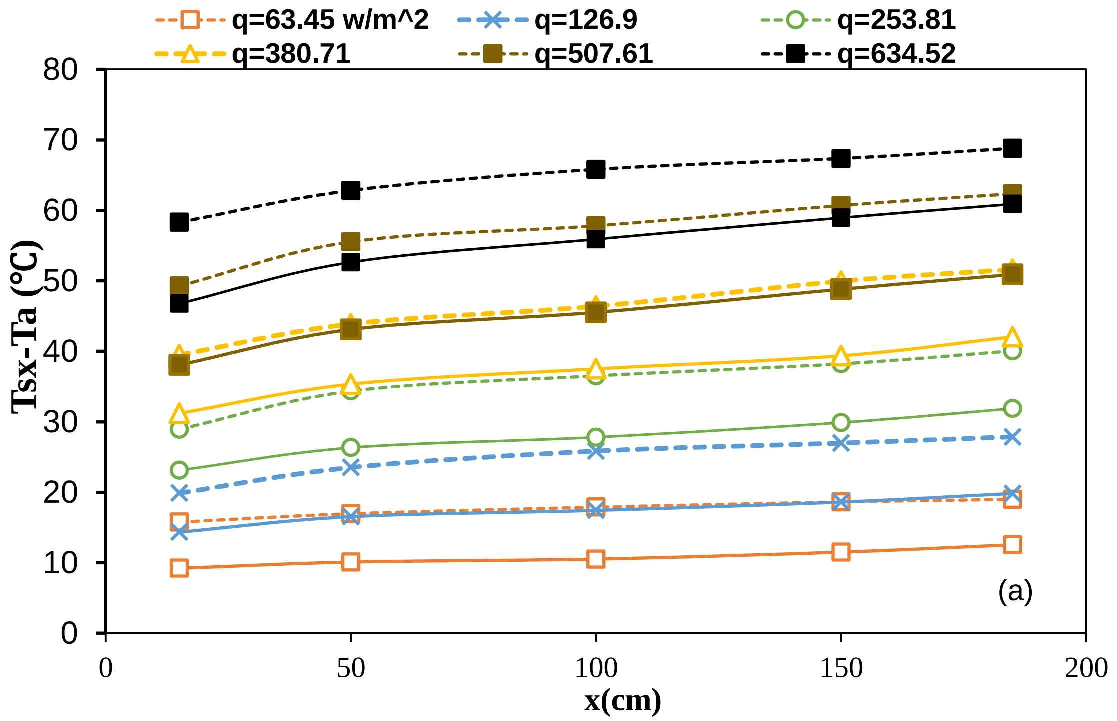
q=63.45 w/m^2
q=126.9
q=253.81
q=380.71
q=507.61
q=634.52
Tsx-Ta (°C)
x(cm)
(a)
0
10
20
30
40
50
60
70
80
0
50
100
150
200

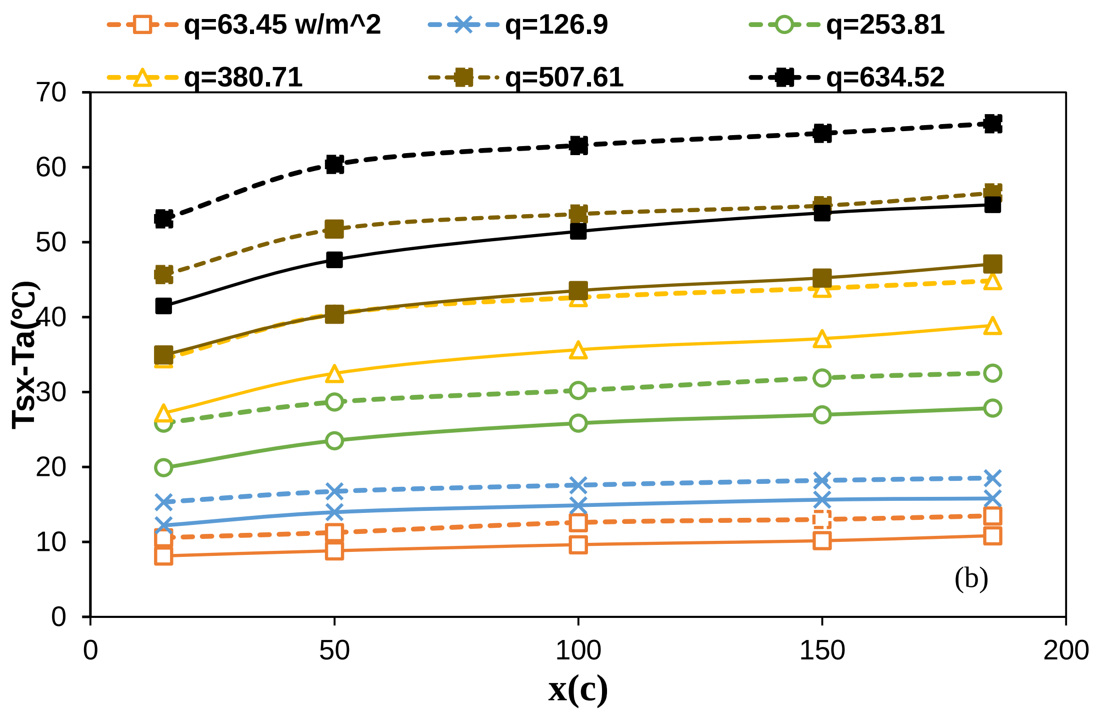
q=63.45 w/m^2
q=126.9
q=253.81
q=380.71
q=507.61
q=634.52
Tsx-Ta(°C)
x(c)
(b)
0
10
20
30
40
50
60
70
0
50
100
150
200

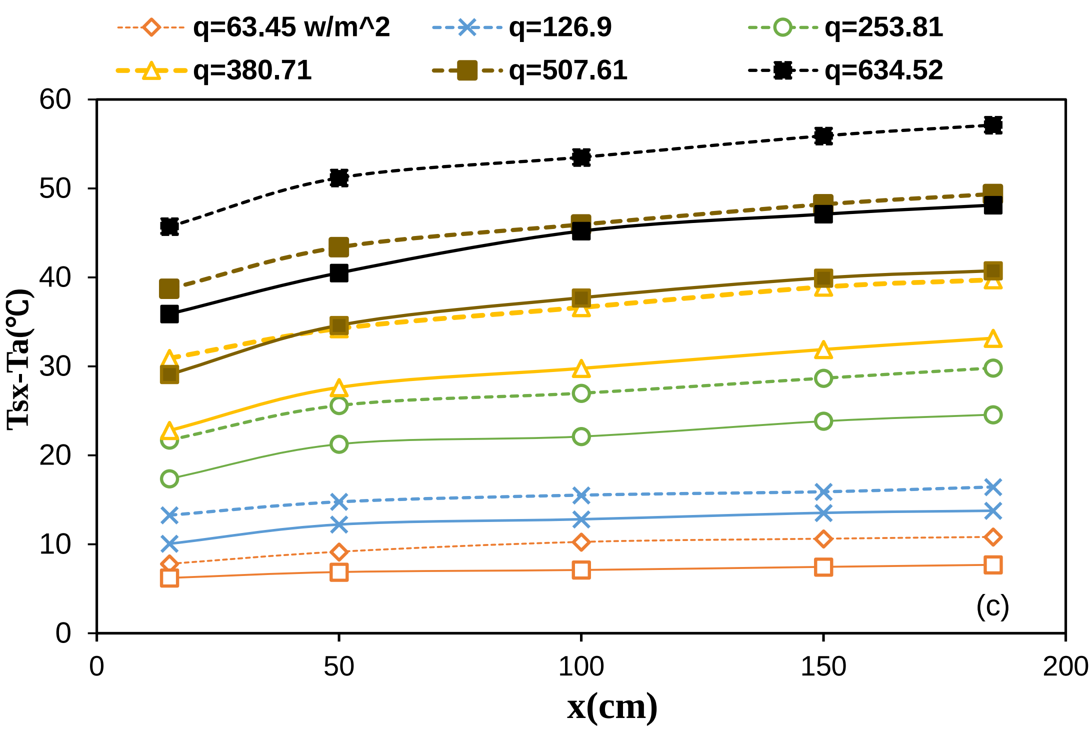

Fig.(8)Temperature difference versus axial distance at different q and θ (The dashed and solid lines represent the results for the smooth and ribbed duct, respectively. (a):30°, (b):45°, (c):60°

local Coefficient of Heat Transfer (h $\frac{W}{m^2.k}$)

Figure (9) illustrates the relationship between the local coefficients of heat transfer (hx) and axial distance (x) for a smooth and ribbed duct at different thermal flux values (q) and inclination angles (θ) of 30°, 45° and 60°. As the axial distance increases, the coefficient of heat transfer (h_x) decreases, indicating that the expansion of the thermal boundary layer along the duct length lessens the efficiency of local heat transfer. Among the three inclination angles, 60° inclination manifests the highest heat transfer performance, followed by 45° and 30°, this is because a bigger inclination angle intensifies the effects of fluid mixing and buoyant forces, which improves natural convection and heat transfer efficiency. The ∨-shaped ribs act as flow disruptors within the duct, creating turbulence and vortices that break the thermal boundary layer formed on the surface of a duct. This minimizes the surface temperature, resulting in a smaller temperature difference. Hence, the transmission of heat is increased, as indicated by the higher heat transfer coefficient, which is inversely proportional to the temperature difference.

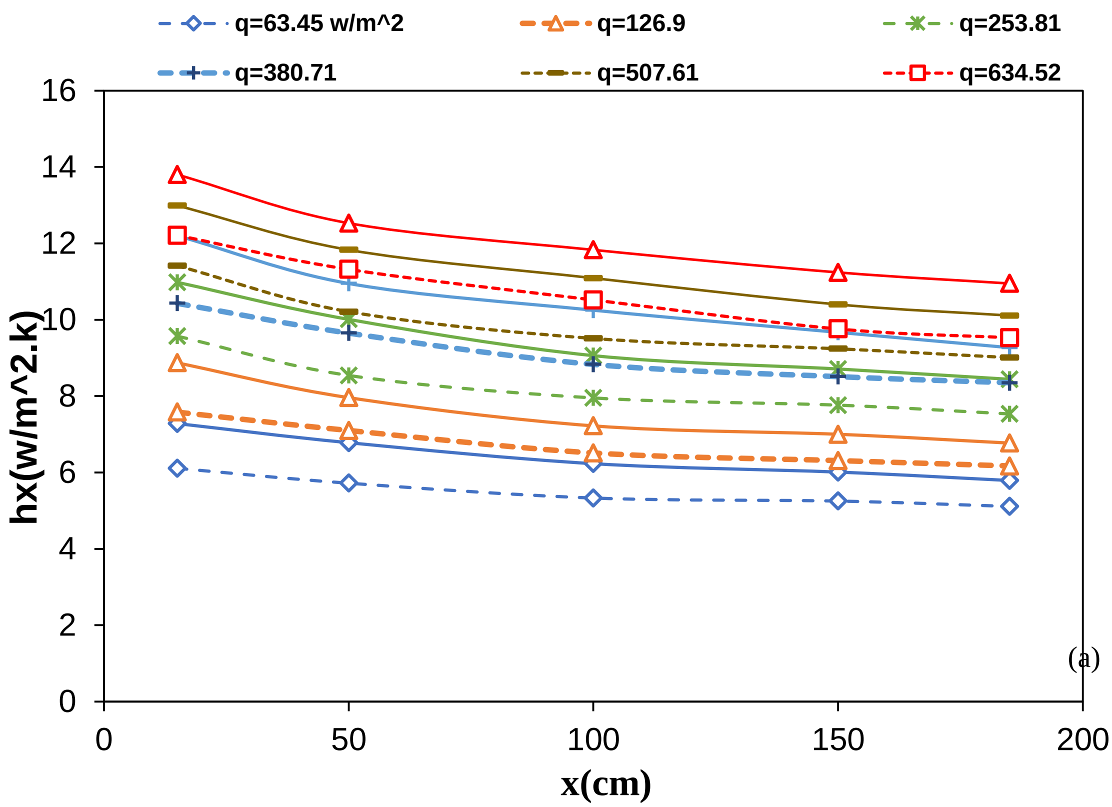
q=63.45 w/m^2
q=126.9
q=253.81
q=380.71
q=507.61
q=634.52
hx(w/m^2.k)
x(cm)
(a)

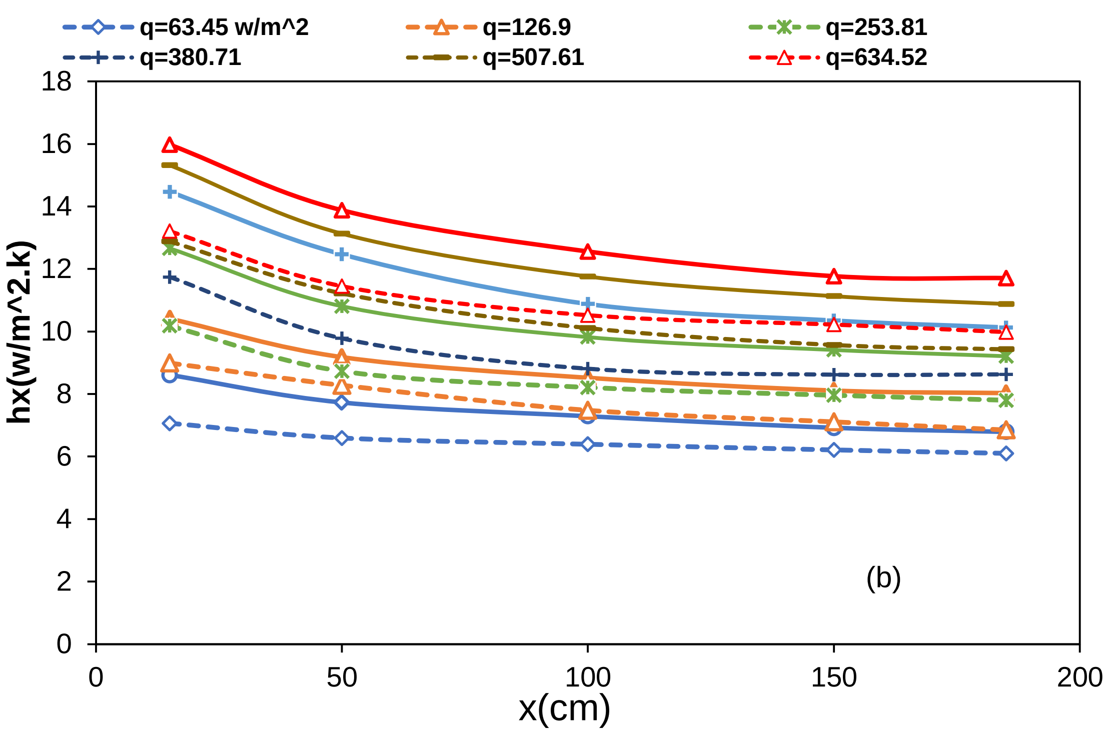
q=63.45 w/m^2
q=126.9
q=253.81
q=380.71
q=507.61
q=634.52
hx(w/m^2.k)
x(cm)
(b)

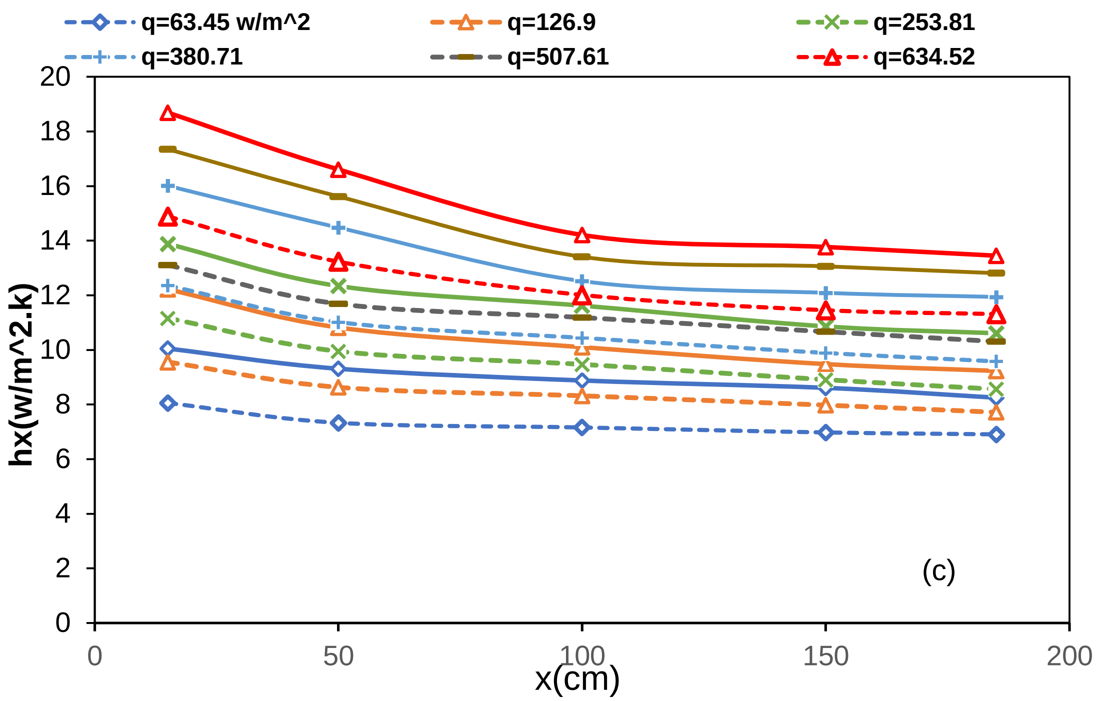

Fig. (9) heat transfer local coefficient vs. axial distance at various q and θ (The dashed and solid lines represent the results for the smooth and ribbed duct, respectively. (a):30^o, (b):45^o, (c):60^o

The Relevance Between Nu$_{av}$ number and Modified Ra Number

Figure (10) illustrates the relationship between the average number of Nusselt and the modified average Rayleigh number (Ra*) for both a smooth and a ribbed duct at three different inclinations (θ =30^o, 45^o and 60^o). The Nu number is generally lower for a smooth duct than a ribbed duct, reflecting the superior heat transfer performance of ribbed surfaces due to increased turbulence and enhanced mixing. Similarly, for a ribbed duct, the 60^o inclination demonstrates the highest Nu$_{av}$, outperforming both the 45^o and 30^o inclinations. The ribbed duct exhibits a noted increase in Nu$_{av}$ compared to the smooth duct for all tested inclination angles, with the 60-ribbed duct achieving the maximum overall heat transfer enhancement. At 30^o, 45^o, and 60^o inclinations, the average number of Nu increases by 21.7%, 32.17%, and 48.15%, respectively.

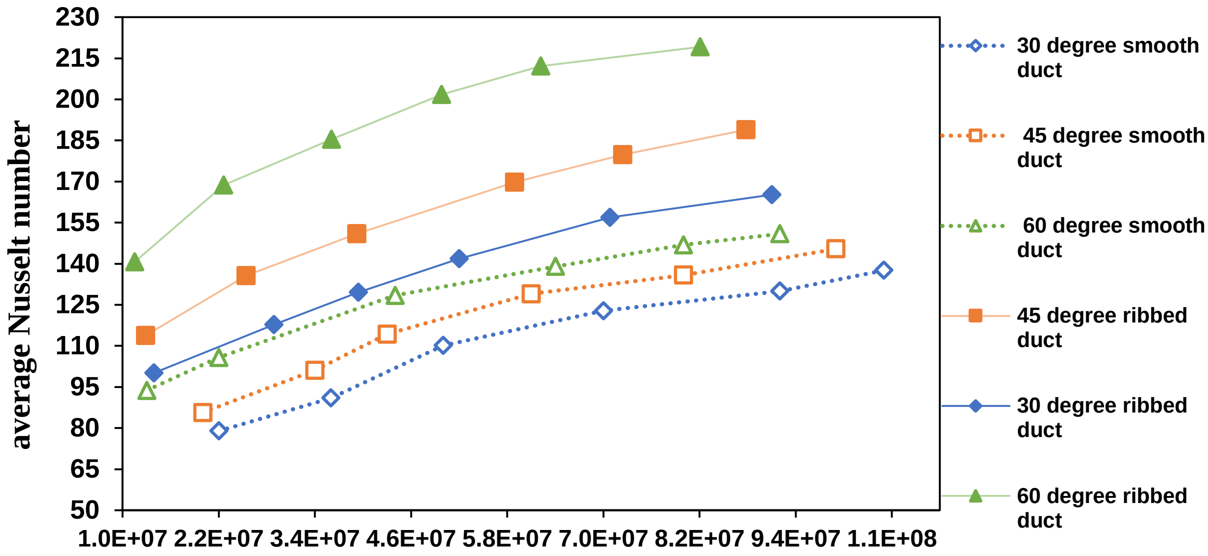

Fig.(10) Average Nu number versus modified Ra number for various q and θ for smooth and ribbed duct

Comparison with the previous results

Figure (11) shows a comparison of the current study with the [Bhushan, T. V. S. M. R., and Reddy, K. V. K., 2015] study. They investigated natural convection heat transfer from inclined square ducts of length 1 m oriented at an angle of 45°. For the smooth duct, both studies exhibit the same trend in which the local heat transfer coefficient decreases as the non-dimensional length increases. This variance between them is due to the difference in boundary conditions and dimensions used. Furthermore, it is clear from the figure that the ribbed duct's local heat transfer coeffici ent values are consistently higher than those of the smooth duct. This suggests that the ribbed surface may facilitate better heat transfer compared to the smooth surface under similar conditions.

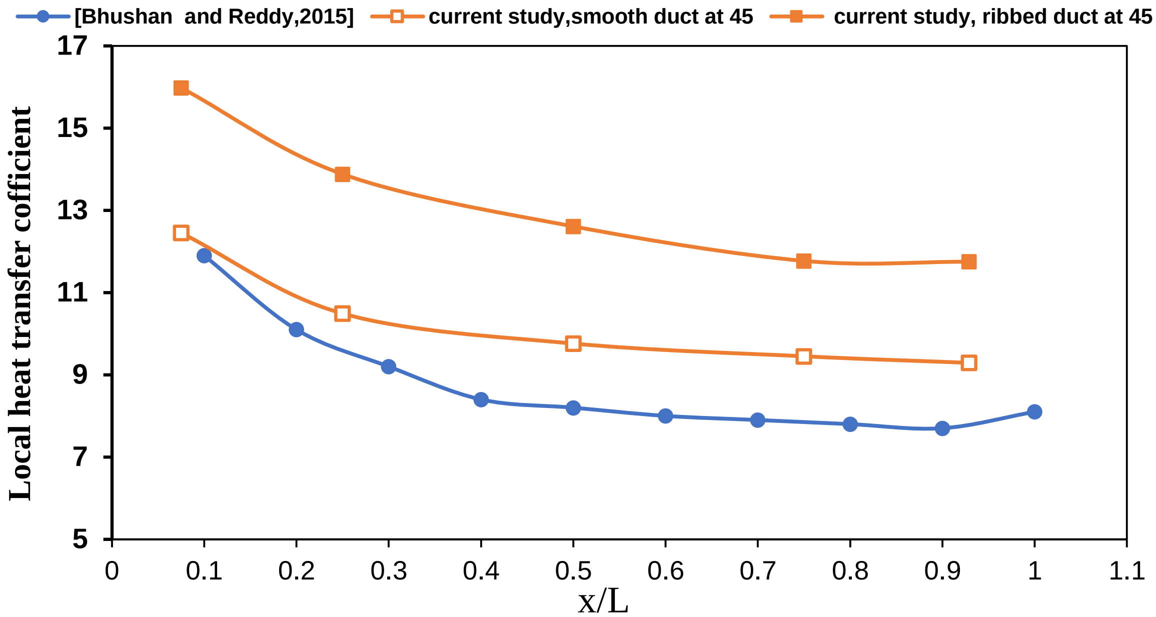

Fig.(11) comparison of the current study with the [Bhushan, and Reddy, 2015] study

CONCLUSION

The study highlights the combined influence of surface geometry (ribbed vs. smooth) and inclination angle (30, 45 and 60 degrees) on heat transfer performance at six thermal fluxes (63.45, 126.9, 253.81, 380.71, 507.61, and 634.52 $\frac{W}{m^2}$). The main outcomes can be summed up as follows:

1. Temperature Distribution: The temperature difference along the axial distance increases due to the thickening of the thermal boundary layer. However, higher inclination angles and the addition of ٧-shaped ribs reduce the temperature difference, improving heat transfer by enhancing buoyancy effects and turbulent mixing.

2. Local Heat Transfer Coefficient (h_x): For smooth duct, (h_x) decreases with axial distance, reflecting the expansion of the thermal boundary layer. Ribbed ducts show significantly higher (h_x), with 60° inclination providing the best performance due to intensified turbulence and improved natural convection.

3. Average number of Nusselt: The ribbed duct outperforms smooth ones in terms of $Nu_{(av)}$, with the 60° ribbed duct achieving the highest heat transfer enhancement by 48.15%.
4. Average Coefficient of Heat Transfer: increasing with increased inclination for both smooth and ribbed duct peakin g at 60°. The ribbed duct exhibits superior h_{av}

compared to smooth ones, owing to their ability to disrupt the boundary layer and generate turbulence.

REFERENCES

Abdelatief, M. A. and Omara, M. A., "Free convection experimental study inside square tube with inner roughened surface at various inclination angles", International Journal of Thermal Sciences, vol. 144, pp. 11–20, 2018, doi: 10.1016/j.ijthermalsci.

Abidi-Saad, A., Polidori, G., Kadja, M., Beaumont, F., Popa, C. V. and Korichi, A., "Experimental investigation of natural convection in a vertical rib-roughened channel with asymmetric heating" , Mechanics Research Communications, vol. 76, pp. 1-10, doi: https://doi.org/10.1016/j.MechanicsResearchCommunications.2016.

Ali, M., "Experimental free convection heat transfer from inclined square cylinders", Heat and Mass Transfer, vol. 53, pp. 1643–1655, 2017, doi: 10.1007/s00231-016-1881-7.

Al-Kayiem, H. H., and Yassen, T. A., "On the natural convection heat transfer in a rectangular passage solar air heater", Solar Energy, vol. 112, pp. 310-318, doi: 10.1016/j.solener.2014.11.031.

Al-Suhaibani, Z., Ali, M., and Almuzaiqer, R., "Tilt Angle Effect on Natural Convection Heat Transfer from an Inclined Array of Square Cylinders" , Energies, vol. 17, pp. 1516, 2024, https://doi.org/10.3390/en17071516.

Baskaya, S., Aktas, M. K., and Onur, N., "Numerical simulation of the effects of plate separation and inclination on heat transfer in buoyancy driven open channels", Heat and Mass Transfer, vol. 35, no. 4, pp. 273–280, 1999, doi: 10.1007/s002310050324.

Bejan, A., Convection Heat Transfer, Fourth Edition, John Wiley and Sons, Inc., USA, 2013.

Bell, S., A beginners guide to uncertainty of Measurement, National Physical Laboratory, Teddington, Middlesex, U.K, 2001.

Bhushan, T. V. S. M. R., and Reddy, K. V. K., "Experimental Investigation on Natural Convection Heat Transfer from Inclined Square Ducts", International Journal of Thermal Technologies, vol. 5, no. 2, pp. 122–126, 2015.

Cengel, Y. A., Heat Transfer: A Practical Approach, 2nd edition, McGraw-Hill, New York, 2002.

Ghani, M. Z., and Salman, Y. K., "Natural Convection Heat Transfer in Inclined Open Annulus Passage Heated from Two Sides", International Journal of Mechanical Engineering and Technology, vol. 5, no. 11, pp. 79–91, 2014.

Gharehghani, A., Hoseini, R., and Salahi, M. M., “Experimental Investigation of Natural Convection Heat Transfer from Horizontal, Inclined and Vertical Cylinders with Constant Heat Flux” , pp. 1-7, 2010, doi: 10.1115/IMECE2010-37903.

Gilani, S. E., Al-Kayiem, H. H., Matthias, B., and Woldemicheal, D. E., “Enhancement of the heat transfer rate in free convection solar air heater”, pp. 12953–12958, 2016.

Hasobee, A. F., and Salman, Y. K., “Natural Convection Heat Transfer Inside Inclined Open Cylinder”, International Journal of Mechanical Engineering and Technology, vol. 5, pp. 92-103, 2014.

Holman, J. P., Heat Transfer, 10th edition, McGraw-Hill Series in Mechanical Engineering, 2010.

Hisham, S. H. , “Performance Enhancement of Air Intake of Gas Turbine Power Plant under the Iraq Environmental Conditions,” Ph.D. dissertation, Mustansiriyah University, Mechanical Engineering Department, Baghdad, August 2023.

Kalendar, A., Oosthuizen, P. H., and Al hadhrami, A., “Experimental study of natural convective heat transfer from an inclined isothermal square cylinder with an exposed top surface mounted on a flat adiabatic base”, pp. 1-8, 2010, doi: 10.1115/IHTC14-22846.

Moawed, M., and Ibrahim, E., “Heat transfer by free convection inside horizontal elliptic tubes with different axis ratios and different orientation angles” , Journal of Renewable Sustainable Energy, vol. 1, no. 1, Aug. 2009, doi: https://doi.org/10.1063/1.3207799.

Mohammed, A. A., Raad, M. A. M., and Ahmed, S., “Natural Convection Heat Transfer in an Inclined Circular Cylinder”, vol. 4, pp. 659-674, 2011.

Naje, W. A., and Hasan, Z. M., “A Review Paper: Study Effect Heat Transfer Convection Natural in a Vertical Channel”, vol. 7, pp. 131-139, Aug. 2022, doi: 10.21608/bfemu.2020.120907.

Nemade, P. D., and Patil, D. R. K., “Effect of Different Geometry and Inclination Angle on Heat Transfer in Natural Convection”, vol. 3, no. 11, pp. 15–20, 2017.

Shehab, S. N., “Natural Convection Properties into a Triangular-Channel: The Orientation and Aspect Ratio Influence”, Journal of Mechanical Engineering Research and Developments, vol. 44, no. 4, pp. 392-399, 2021.

Shehab, S. N., “Study of Baffles Arrangement Influence on the Natural Convection into a Heated Square Channel”, Mathematical Modelling of Engineering Problems, vol. 9, no. 4, pp. 1025-1030, 2022, doi: 10.18280/mmep.090420.

Appendix(A)

calibration procedure:

Thermometer readings **Thermocouple readings**

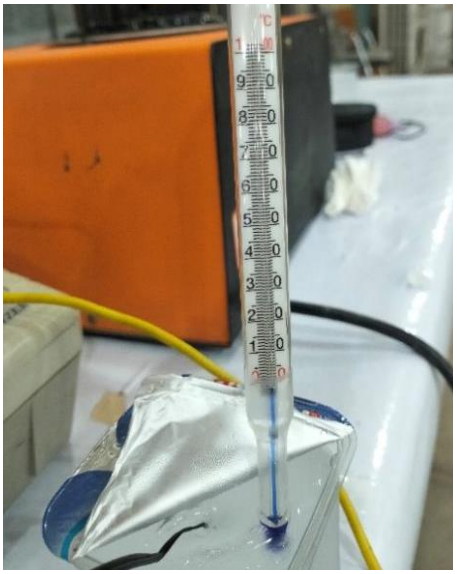

Iced water

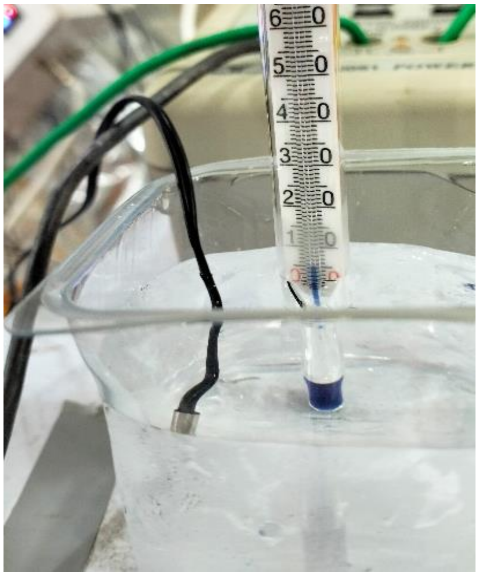

Cold water

Warm water

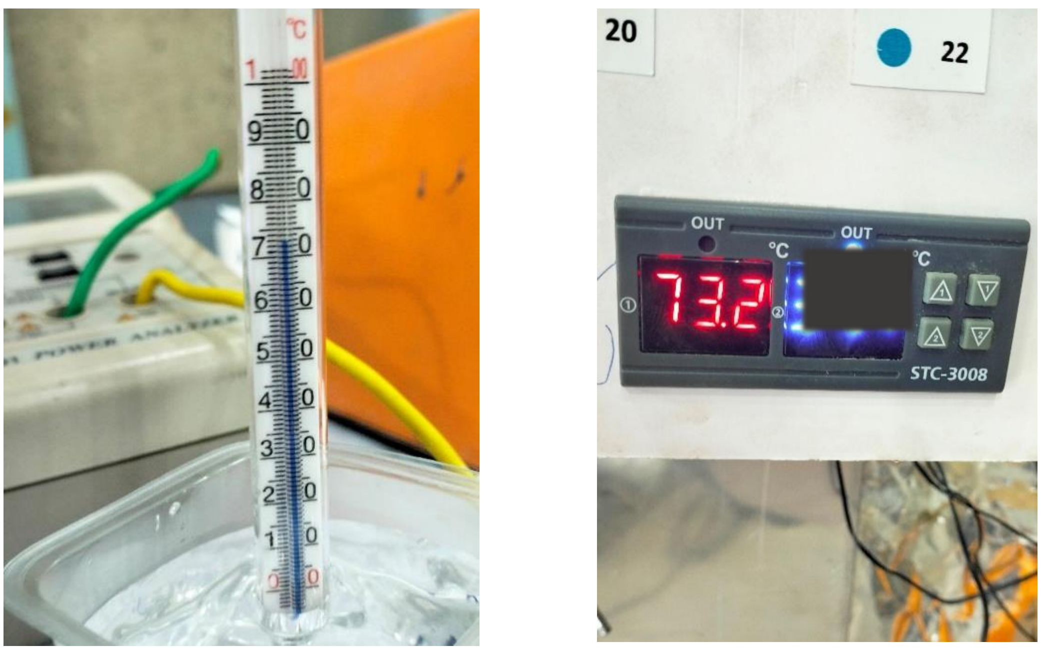

Hot water

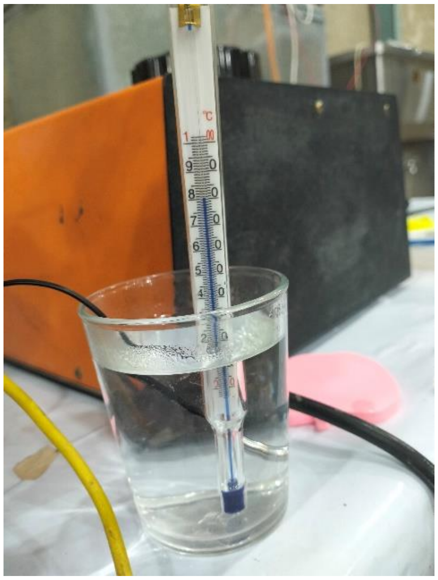

Boiling water